Precipitation estimate of a heavy rain event using a C-band solid-state polarimetric radar

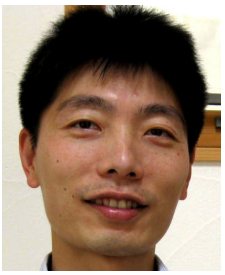

Hiroshi Yamauchi

Hiroshi Yamauchi[1], Ahoro Adachi[1], Osamu Suzuki[2], Takahisa Kobayashi[3]
[1]*Meteorological Research Institute, Tsukuba, Japan, hyamauch@mri-jma.go.jp*
[2]*Japan Meteorological Agency, Tokyo, Japan*
[3]*Central Research Institute of Electric Power Industry, Abiko, Japan*
(Dated: 30 May 2012)

1. Introduction

Improving monitoring and forecasting system for local heavy rainfalls in urban area have become an urgent issue in Japan. Since urban area covered by concrete has little space to keep rain water, even several 10 minutes of local heavy rainfall causes surge of water level in small rivers, drainages, depressions, which sometimes brings on casualties. To issue weather warning for such kind of disaster with an enough lead time, we need to capture three dimensional structure of local heavy rainfall with high accuracy, with high temporal and spatial resolutions. Polarimetic radar is suitable for observing local heavy rainfall for its capabilities to estimate rain rate with high accuracy. However, polarimetric radar tends to need longer observation time than conventional radar because it needs larger sample number to ensure quality of measurement.

This issue could be mitigated by adoption of solid-state transmitters for polarimetric radar. Stable transmitting wave emitted by solid-state transmitter enables accurate polarimetric observation with small sample number.

Here, we report validation result of rainfall estimates with the C-band solid-state polarimetric radar of Meteorological Research Institute (hereinafter, MRI radar) using disdrometer observations for a record heavy rainfall event.

2. Data and Methodology

In the afternoon of 26th August, 2011, Tokyo metropolitan area experienced a record heavy rainfall. The Nerima weather station of Japan Meteorological Agency observed hourly accumulation rainfall of 90.2 mm. This heavy rainfall event was observed by the MRI radar located 50 km northeast in Tokyo and an optical disdrometer located in Itabashi, Tokyo.

2.1 MRI C-band solid-state polarimetric radar

Table 1 summarizes specifications and operating parameters of the MRI radar. Details of the radar are described in Wada et al (2009). The uniqueness of this radar is adoption of solid-state transmitters. The peak power of the solid-state transmitter

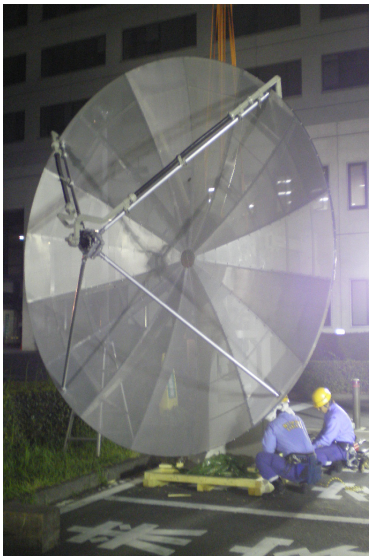

Fig. 1 Antenna of the MRI radar

Table 1. Specifications and operating parameters of the MRI radar

Frequency		5370 MHz
Transmitters		GeAs Power FET
Peak Power		3.5 kW for both horizontal and vertical transmitters.
Antenna diameter		4 m (parabolic, Fig. 1)
Beam width		< 1°
Antenna gain		> 42 dB
Signal min.		< -110 dBm
Range gate spacing		150 m
Radome diameter		7 m
Antenna speed	(EL < 8°)	4 rpm (Maximum 10 rpm)
	(EL >= 8°)	6 rpm
Sample (hit) number		20
Azimuth spacing		0.7°
PRF	(EL < 8°)	624 / 780 Hz
	(EL >= 8°)	936 / 1170 Hz
Pulse width	(EL < 8°)	1 μs (range < 20km), 129 μs (range >= 20km)
	(EL >= 8°)	1 μs (range < 7.5km), 63 μs (range >= 7.5km)
Transmitting mode		Simultaneous
Observation parameters		Zhh, Zvv, Vd, velocity width, ρhv, Φdp

is about a hundredth of that of conventional transmitter such as magnetron and klystron. To achieve the same sensitivity and radial resolution as radar with conventional transmitter, the radar uses long pulses with FM chirp and pulse compression technique. To observe blind range of long pulse observation, the dual-cycle observation technique (Nakagawa et al 2005) which alternately execute short pulse (1μsec) observation and long pulse observation is used.

Adoption of solid-state transmitters brings several advantages such as narrow bandwidth, no need of high voltage components, high redundancy and low operational cost. One of the most important advantages is high precision of polariemtric parameters. Figure 2 shows the distribution of ρhv for samples collected in stratiform rain with SNR larger than 20dB by the MRI radar. Peak values of ρhv are 0.998 and 0.992 for long and short pulse observations, respectively. The distribution seems almost independent of sample number N. Figure. 3 shows the distribution of standard deviation of Φdp calculated using nine gate windows along radial. Peak values of Φdp are 1.0° and 2.0° for long and short pulse observations, respectively. As is the case with ρhv, the distribution seems independent of sample number N.

By virtue of the high precision with small sample number, the radar can observe polarimetric parameters with practical antenna scan speeds of 4 rpm for low elevation angle (EL < 8) and 6 rpm with high PRF for high elevation angle (EL >= 8°). This enables us to conduct volume scan with 13 elevations of PPI and 2 azimuths of RHI every 4 minutes. The lowest elevation PPI scan (EL=0.5°) is conducted every 2 minutes.

Disadvantage of solid-state radar is range side-lobe (time side-lobe) which is imperative in using pulse compression technique. However, level of range side-lobe is small. Figure 4 shows a sample of reflectivity of range side-lobe for a strong aircraft echo observed by vertical pointing PPI. Range side-lobes appear in both front and back of the aircraft echo. Figure 5 shows signal power profile of the range side-lobes along radial. The suppression level is about -50dB which is slightly worse than that of azimuthal side-lobe caused by antenna beam pattern.

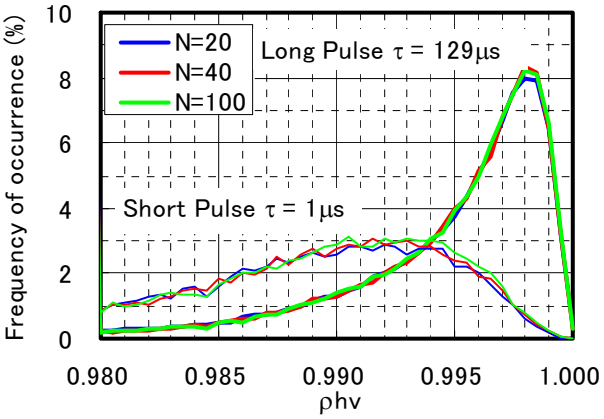

Fig .2 Distribution of ρhv for samples collected in stratiform rain with SNR larger than 20dB by the MRI radar.

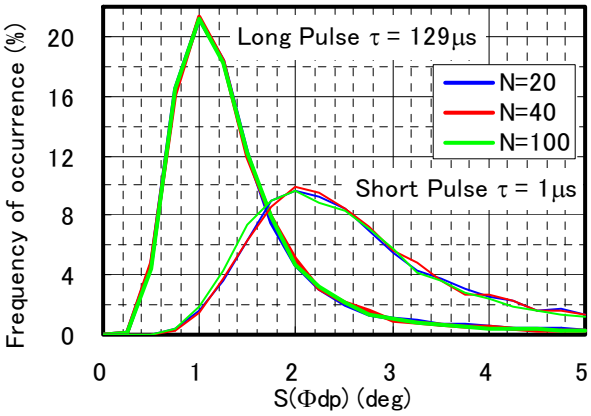

Fig .3 Distribution of the standard deviation of Φdp for samples collected in stratiform rain with SNR larger than 20dB by the MRI radar.

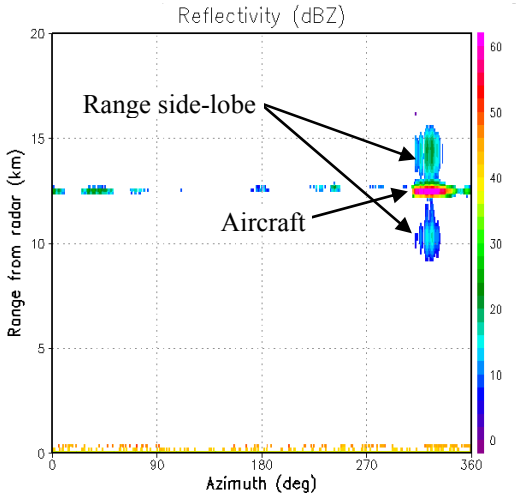

Fig. 4 Sample reflectivity field of range side-lobe for a strong aircraft echo.

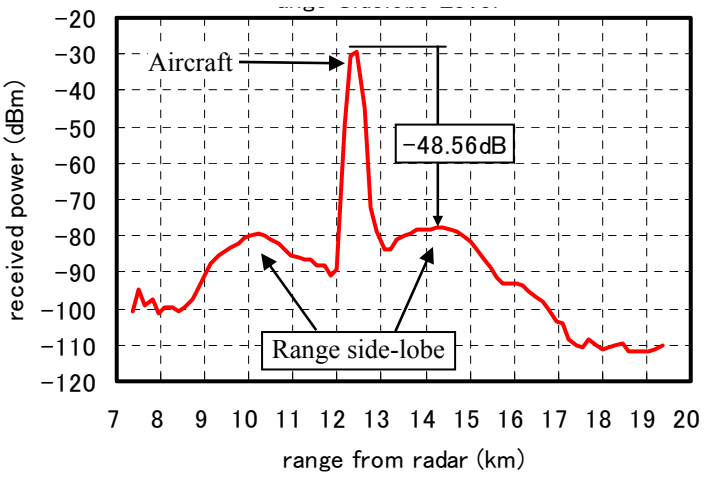

Fig. 5 Signal power profile of range side-lobe along radial.

Differential scattering phase δ is removed from differential phase Φdp using IIR filtering method proposed by Hubbert and Bringi (1995). Then specific differential phase Kdp is derived from the Φdp using the method proposed by Savitzky and Golay (1964). Attenuation corrected reflectivity Z_corr is derived from reflectivity Z and Φdp according to the following equation:

Z_corr = Z + 0.073 Φdp (Bringi and Chandrasekar 2001)

Rain rate R(Kdp, Z_corr) is estimated as follows:

(Kdp < 1 °km^{-1} or Z_corr < 30dBZ) R(KDP, Z_corr) = R(Z_corr) = 0.0365 Z_corr$^{0.625}$ (Marshall and Palmer, 1948)

(Kdp >= 1 °km^{-1} and Z_corr >= 30dBZ) R(KDP, Z_corr) = R(KDP) = 129 Kdp$^{0.85}$ (Bringi and Chandrasekar 2001)

2.2 Optical disdrometer

We installed an optical disdrometer (Löffler-Mang and Joss, 2000) at our observation site in Itabashi, Tokyo (hereinafter Itabashi site). The distance between Itabashi site and the radar site is 52 km. The height of the beam center of the lowest elevation PPI is 600 m at this site.

The disdometer outputs raindrop size – velocity distribution for specified time period. The distribution was recorded every minute. The data with less velocity than the half or twice of the terminal velocity (Gunn and Kinzer, 1949) are removed. After the quality check, reflectivity Z(Disdro) and rain rate R(Disdro) are calculated from the distribution.

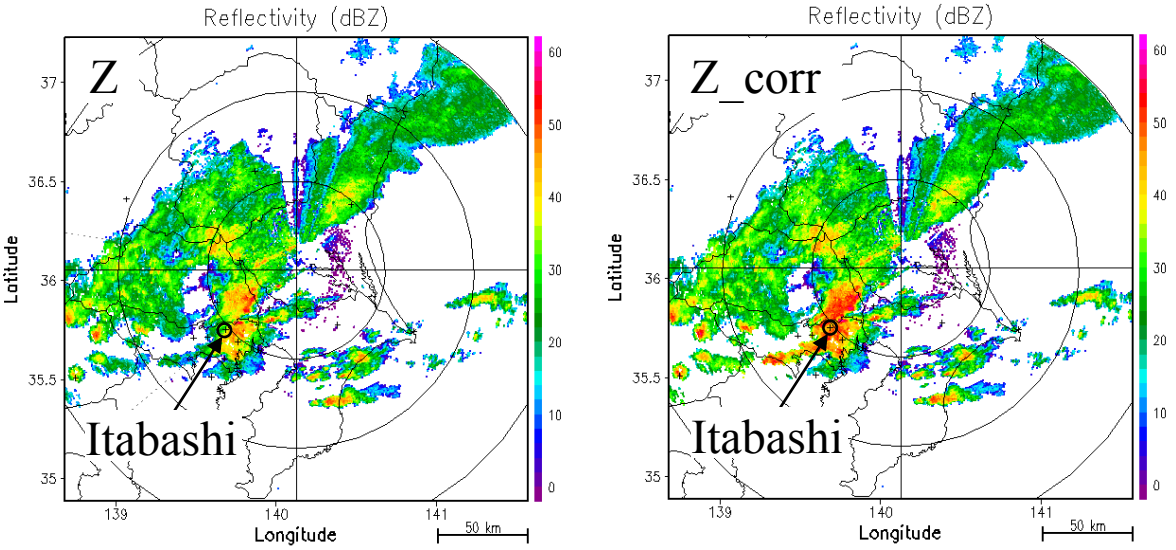

Fig. 6 Reflectivity fields without attenuation correction (left) and with attenuation correction (right) observed by the MRI radar at elevation angle of 0.5° at 15:21 LST.

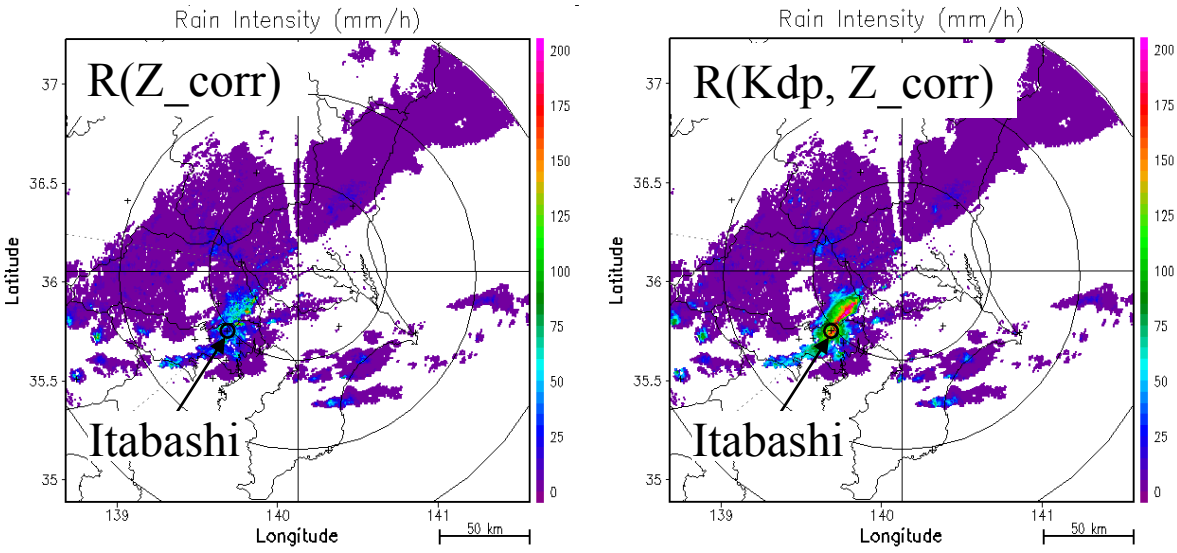

Fig. 7 Sample of rain-rate fields estimated from Z-R relation (left) and estimated using specific differential phase (right) observed by the MRI radar at elevation angle of 0.5° at 15:21 LST..

3. Results

Figure 6 shows the reflectivity fields observed by the MRI radar at 15:21LST on 26th August 2011. At this time Tokyo metropolitan area located southwest of the radar experienced heavy rainfall. The reflectivity in the heavy rainfall area is significantly changed by the attenuation correction. Figure 7 is rain rate distributions at the same time with Figure 6. The left figure shows rain rate distribution estimated using corrected Z and Z-R relation (R(Z_corr)) and the right figure shows rain rate distribution of R(Kdp, Z_corr). R(Kdp, Z_corr) indicates much higher value than R(Z_corr) in Tokyo metropolitan area.

Reflectivity and rain rate obtained by the radar were compared with those measured by the disdrometer over radar pixel centered on the disdrometer location. Since sampling volume of radar observation locates hundreds of meters aloft, the comparison have to consider fall times of raindrops. We assumed fall time was 3 minutes and shifted 3 minutes to radar observation time.

Figure 8 shows the time series of reflectivity at the Itabashi site measured by disdrometer, Z(Disdro), observed by the MRI radar with attenuation correction, Z_corr, and without correction, Z. While Z is significantly less than Z(Disdro), Z_corr is similar to Z(Disdro) except the period of 15:10 to 15:30 when Z(Disdro) is more than 50 dBZ.

Figure 9 shows the time series of rain rate measured by the disdrometer, R(Disdro), estimated from reflectivity without correction, R(Z), estimated from reflectivity with correction, R(Z_corr), and estimated from Kdp and Z_corr, R(Kdp, Z_corr). The disdrometer measured strong rain rates of more than 100mmh^{-1} over 12 minutes, reaching as much as 160 mmh^{-1}. The hourly accumulation of R(Disdro) from 15:00 to 16:00 is 63mm.

R(Kdp, Z_corr) agrees well with R(Disdro), while R(Z) and R(Z_corr) are quite different from R(Disdro). The hourly accumulation of R(Kdp, Z_corr) agrees well with that of R(Disdro) (9% overestimated). On the other hand, the hourly accumulation of R(Z) and R(Z_corr) are 84% and 44% underestimated, respectively.

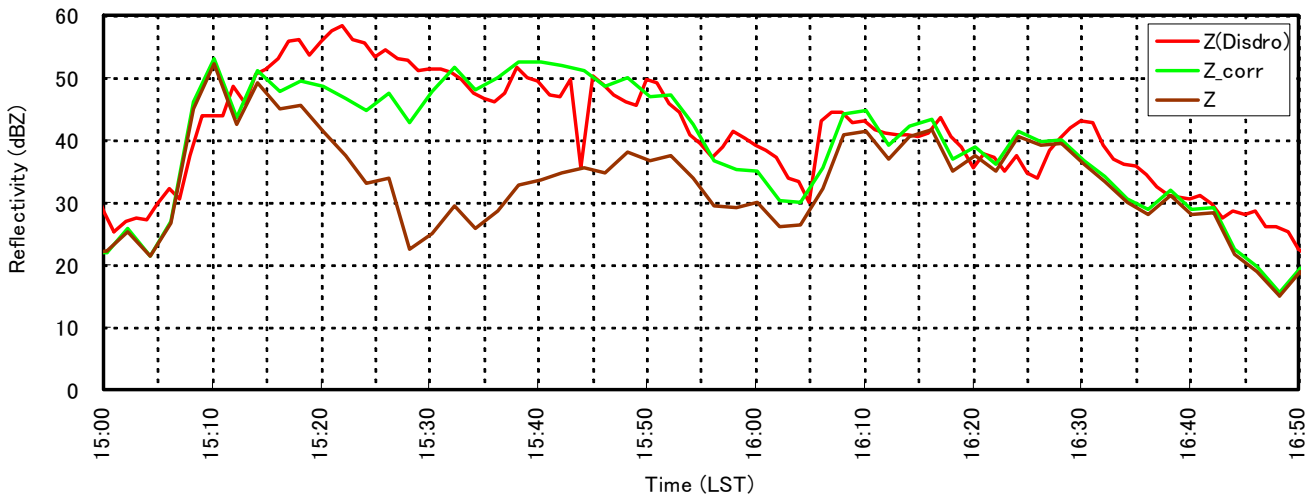

Fig. 8 Time series of reflectivity at the Itabashi site measured by disdrometer (red), observed by the MRI radar with attenuation correction (green) and without correction (brown).

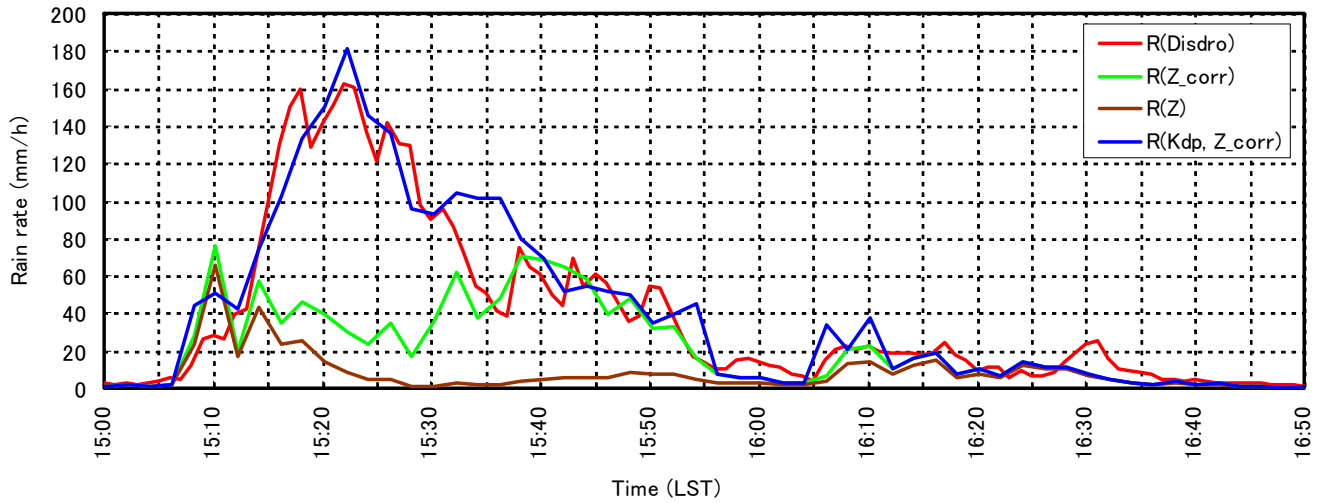

Fig. 9 Time series of rain rate at the Itabashi site measured by disdrometer (red), esteimated using Z_corr (green), esteimated using Z (brown) and estimated using polarimetric parameters R(Kdp, Z_corr).

4. Summaries and conclusions

A local heavy rainfall occurred in Tokyo metropolitan area on 26th August, 2011. An optical disdrometer of the Itabashi site located 52km away from the radar site observe strong rain rates of more than 100mmh^{-1} over 12 minutes and hourly accumulation rainfall of 63 mm. Rainfall estimates of the MRI radar over radar pixel centered on the disdrometer location were validated using this disdrometer observation. Time series of reflectivity with attenuation correction agrees well with that of the disdrometer, if reflectivity is less than 50 dBZ. Time series of rain rate estimated using Z-R relation is far from that of the disdrimeter. On the other hand, time series of rain rate estimated from Kdp agrees well with that of the disdrometer. The hourly accumulation of rain rate estimated from Z-R relation is 84% underestimated, while the estimation from Kdp is only 9 % overestimated.

Owing to adoption of solid-state transmitters, the MRI radar can observe polarimetric parameters with high precision with small sample number. The peak values of ρhv and the standard deviation of Φdp for stratiform rain are 0.998 and 1.0°, respectively. This result shows that C-band solid-state polarimetric radar has sufficient capability, in order to observe heavy rainfall with a practical scanning rate.

Acknowledgment

This study is partially supported by the Japan Science and Technology Agency.

References

Bringi, V.N., and Chandrasekar, V., 2001: Polarimetric Doppler Weather Radar: Principles and Applications, Cambridge University Press, pp 636.

Gunn, R., and Kinzer, G. D., 1949: The terminal velocity of fall for water drops in stagnant air. *J. Meteor.,* **6**, 243–248.

Hubbert, J., and Bringi, V.N., 1995: An iterative filtering technique for the analysis of copolar differential phase and dual-frequency radar measurements. *J. Atmos. Oceanic Technol.*, **12**, 643-648.

Löffler-Mang, M., and Joss, J., 2000: An optical disdrometer for measuring size and velocity of hydrometeors. *J. Atmos. Oceanic Technol.,* **17**, 130–139.

Marshall, R. E., and Palmer, W. McK., 1948: The distribution of raindrops with size. *J. Meteor.*, **5**, 165-166.

Nakagawa, K., Hanado, H., Fukutani, K., and Iguchi, T., 2005: Development of a C-band pulse compression weather radar. extended abstract, *32nd Conf. on Radar Meteorology*, Albuquerque, U.S, Amer. Meteor. Soc., P12R.11.

Savitzky, A.; and Golay, M.J.E., 1964: Smoothing and Differentiation of Data by Simplified Least Squares Procedures. Analytical Chemistry **36**, 8, 1627–1639.

Wada, M., Horikomi, J., and Mizutani, F., 2009: Development of solid-state weather radar. preprints, *34th Conf. on Radar Meteorology*, Williamsburg, VA, U.S, Amer. Meteor. Soc., 12B.4.